Remote Reconfiguration of Microwave Filters Using Dielectric Tuners

Abhishek Sharma, Javier Ossorio, Davide Smacchia, Tillmann Tronser, Santiago Cogollos, *Member, IEEE*, Vicente E. Boria, *Fellow, IEEE*, and Marco Guglielmi, *Life Fellow, IEEE*

***Abstract*— The objective of this article is to explore the use of dielectrics to reconfigure remotely microwave filters in rectangular waveguide. To start, we study experimentally the phase shift that is achievable using dielectric tuning elements in a rectangular waveguide. We then compare the results obtained with the performance of standard metallic tuning cylinders and screws. Next, the passive intermodulation (PIM) behavior of dielectric tuning elements is investigated experimentally. The PIM results obtained using dielectrics are then compared with the ones of metallic tuning elements. After that, the measured results for a filter tuned with a number of different dielectric tuning elements are discussed to identify the required relation between cavity size, dielectric constant, and tuner diameter. As a proof of concept, we then design, manufacture, and test two filters, one in WR75 and the other in WR90. Both simulated and measured results are then presented clearly demonstrating that the structures discussed can indeed be reconfigured (or tuned) both in terms of filter center frequency and bandwidth. Finally, computer-driven linear actuators are connected to the dielectric tuners, and the remote tuning capability is successfully demonstrated.**

***Index Terms*— Dielectric tuners, linear actuators, microwave filters, passive intermodulation (PIM), reconfigurable filters, rectangular waveguide, remote tuning.**

I. Introduction

METALLIC tuning elements or screws have traditionally been used in many different types of microwave filters in rectangular waveguide to compensate for both design and manufacturing inaccuracies [1], [2].

Although the recent availability of accurate full-wave simulation tools has enabled the development of accurate filter design and tuning procedures [3], [4], tuning elements (or screws) are still widely used today to recover the effects of manufacturing errors in sensitive devices as discussed in [5] for combline topology and in [6] and [7] for dual-mode filters. Furthermore, tuning screws can also be utilized to allow for the use of low-cost manufacturing techniques with significant tolerances, as discussed in [8], and to compensate for temperature variations [9], [10].

Another popular use of metallic tuning elements is to design filters that can produce different responses using the same filter body for low-cost high-volume productions [11], [12], [13]. Adjustable cylindrical metallic inserts are also very frequently used in evanescent-mode filters [14]. As shown in [15], tuning screws can conveniently be used to implement both tunable resonators and adjustable couplings.

Significant effort has also been devoted in the past to the development of dedicated computer-aided design (CAD) models for the accurate simulation of tuning elements in rectangular waveguide filters [13], [16], in circular waveguide dual-mode filters [17], [18], [19], and in combline filters [20].

Finally, it is important to recall that microwave filters are normally designed to operate at a single center frequency, and with a fixed bandwidth. Recently, however, the constant demand of modern communication services for more agility and bandwidth is radically changing filter requirements [21]. To satisfy the new demands, therefore, metallic screws have also been recently proposed to implement microwave filters that can be tuned over a wide frequency range [22], [23], [24]. In this context, more recent contributions propose the use of new structures, where tuning element are used only in the resonators, thus implementing simpler filter structures, where only the center frequency can be tuned and the bandwidth remains constant [25], [26].

It is important to note, however, the use of metallic tuning screws introduces several drawbacks. One of them is that they are very sensitive elements and a very small variation in depth can cause an important effect in the filter response (especially for resonators). They can also reduce the power-handling capability due to undesired high-power effects [27], [28], [29]. In addition, the use of metallic tuning elements, or screws, requires a nut that needs to be fastened to the filter body to ensure good electrical contact and to fix precisely the tuner in the desired position. As a consequence, the use of metallic tuning elements can result into bulky and complex implementations if remotely tunable filters are required, as in [30] and [31].

In addition to metallic tuning screws, however, it is also possible to tune microwave filters with dielectric tuning elements. Furthermore, dielectric resonators are also commonly used for

Manuscript received 2 December 2022; accepted 27 December 2022. Date of publication 6 February 2023; date of current version 30 June 2023. This work was supported in part by the European Union's Horizon 2020 Research and Innovation Program, through the Marie Skłodowska-Curie ITN (TESLA) under Grant 811232 and in part by the Minsiterio de Ciencia e Innovación (MICIN, Spanish Government) through the Research and Development Project under Grant PID2019-103982RB-C41 (funded by MICIN/AEI/10.13039/501100011033). *(Corresponding author: Abhishek Sharma.)*

Abhishek Sharma, Santiago Cogollos, Vicente E. Boria, and Marco Guglielmi are with ITEAM, Universitat Politecnica de Valencia, 46022 Valencia, Spain (e-mail: asharma@iteam.upv.es; sancobo@dcom.upv.es; vboria@dcom.upv.es; marco.guglielmi@iteam.upv.es).

Javier Ossorio and Davide Smacchia are with the Val Space Consortium, European Space Agency (ESA), 46022 Valencia, Spain (e-mail: javier.ossorio@val-space.com; davide.smacchia@val-space.com).

Tillmann Tronser is with Tronser GmbH, 75331 Engelsbrand, Germany (e-mail: tillmann@tronser.com).

Color versions of one or more figures in this article are available at https://doi.org/10.1109/TMTT.2023.3238770.

Digital Object Identifier 10.1109/TMTT.2023.3238770

implementing small-size high-performance microwave filters [32], [33].

Although dielectric rods and screws can indeed be found in the market, their use as tuning elements in waveguide filters has not been discussed in detail in the technical literature. To the author's knowledge, only a few encouraging initial results have been published in the recent past in [34], [35], and [36], and more recently in [37].

In this context, therefore, the objective of this article is to contribute to the state-of-the art of reconfigurable filters based on dielectric tuners by discussing in detail the following aspects.

1) We report the results of an experimental investigation exploring the tuning behavior of a number of dielectric and metallic tuning elements.
2) We also discuss the different behavior of smooth and threaded (screws) tuning elements.
3) Furthermore, the passive intermodulation (PIM) behavior for both metallic and dielectric tuning elements is explored with a number of experiments.
4) The measured results of a microwave filter tuned with a number of different dielectric tuning rods, changing both dielectric constants and rod diameters, is also reported.
5) In addition, we also carry out an experimental investigation to explore the optimal sizes and dielectric constant of the dielectric tuning element to achieve the best tuning performance.
6) Furthermore, we also discuss the design, fabrication, and measurement of two dielectric-tuned filters, one in WR75 and the other in WR90.
7) In addition to tunable center frequency, we also successfully demonstrate, with both simulation and measurements, the possibility of tuning the filter bandwidth.
8) Finally, we successfully prove the viability of the concept of remote reconfiguration a microwave filter in rectangular waveguide with the use of computer-controlled, low-cost, piezoelectric linear actuators.

II. Phase Shift Experiments

The starting point of our investigation is the experimental evaluation of the maximum phase shift that can be introduced by metallic or dielectric tuning elements in a rectangular waveguide. It is important to note, however, that an alternative would have been to build a one pole resonator and measure the actual shift in frequency as a result of the changes in tuning element penetration. The choice of the phase shift measurement, instead of measuring the frequency shift of a resonator, has been dictated by the need to perform in addition an experimental investigation of the PIM behavior, as described in Section III. In any case, as explained in Section III-A, the phase shift introduced by a tuning element can be directly related to the change in frequency of a resonator that contains the same tuning element.

The device that we have used to measure the maximum phase shift introduced by tuning elements is composed of two identical lengths of WR75 waveguide [device under tests (DUTs)], as shown in Fig. 1. Both DUTs have been built using

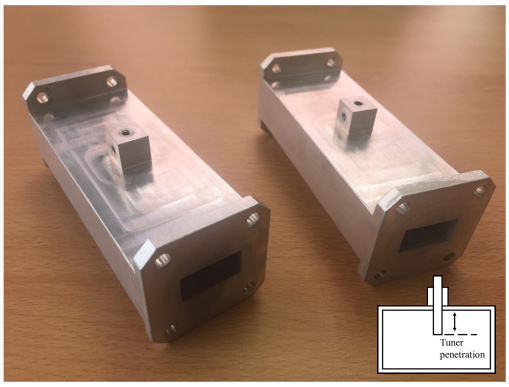

Fig. 1. Lengths of WR75 waveguide (100 mm). Note the hole for the lateral fixing screw on the small cube on top of the waveguides. The insert in the bottom right corner shows the cross section of the DUTs at the location of the tuning element.

aluminum and spark erosion, and have a hole of 3.0 mm in diameter in the center of the upper wall. However, in one of the DUTs the hole is smooth, while, in the other, the hole is threaded with the M3 standard. One important detail concerning the structure of the DUT is the choice of the diameter and location of the hole. The diameter is chosen so that the circular waveguide that is introduced (the hole itself) is below cutoff in the frequency range of interest. The second is that locating the hole in the center of the upper waveguide wall, we avoid the excitation of the modes of the circular waveguide. Both features actively contribute to the elimination of power leakage from the DUTs. This is indeed an important consideration for the filter implementations discussed later in this article. This feature, in particular, is one of the aspects that distinguishes our solution from other approaches discussed in the technical literature, where special attention must be paid to the suppression of unwanted leakage from tunable filters thus resulting in more complex implementations [38], [39], [40], [41].

Using our DUTs, we have then measured the phase shift introduced as a function of frequency for the following cases.

1) Smooth aluminum rod $\sigma = 3.56 \times 10^7$ S/m.
2) Smooth stainless steel (SS) rod $\sigma = 6.993 \times 10^6$ S/m.
3) Smooth Teflon rod $\epsilon_r = 2.1$, $\tan\delta = 0.0002$.
4) Smooth Sapphire rod $\epsilon_r = 9.3$, $\tan\delta = 0.0004$.
5) Threaded aluminum rod $\sigma = 3.56 \times 10^7$ S/m.
6) Threaded SS rod $\sigma = 6.993 \times 10^6$ S/m.
7) Threaded Teflon rod $\epsilon_r = 2.1$, $\tan\delta = 0.0002$.

Fig. 2 shows the tuners that we have manufactured. To perform the actual measurement, the two DUTs have been connected in cascade, with a 10-mm silver-plated joining waveguide section. This was done to perform all necessary measurements without disconnecting the DUTs from the vector network analyzer (VNA). Furthermore, in each case, the tuning element was inserted to the maximum possible penetration before the appearance of the resonance introduced by the tuning element itself.

The phase shift curves that we present have been obtained computing the difference in the phase of S_{21} between the measurement with the tuner and the measurement without the tuner. In all cases, the measurement setup included a

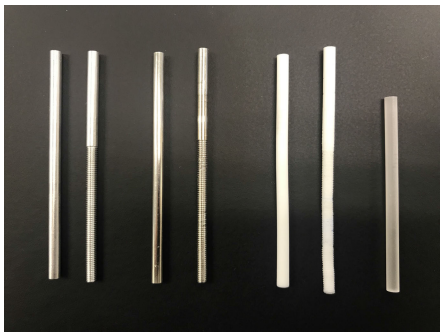

Fig. 2. Tuners used for the insertion phase measurements. From the left: Aluminum, SS, Teflon, Sapphire. All rods have 3-mm diameter. The total length of the metallic and teflon rods is 50 mm and length of sapphire rod is 40 mm.

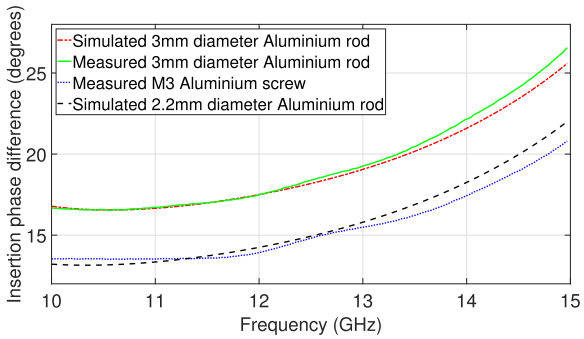

Fig. 3. Aluminum tuners. Top: smooth rod and bottom: threaded. The simulated result have been obtained with CST design studio.

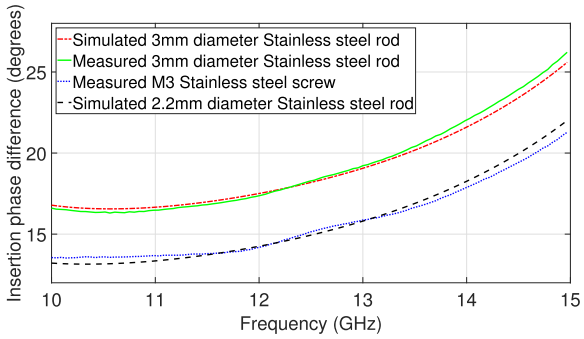

Fig. 4. SS tuners. Top: smooth rod and bottom: threaded. The simulated result have been obtained with CST design studio.

VNA with two coaxial to WR75 transitions. A standard technology readiness level (TRL) calibration was performed with reference planes at the end of the coaxial to WR75 transitions.

Fig. 3 shows the results obtained with the aluminum tuners penetrating 3 mm. It is interesting to note that the threaded tuner introduces less phase shift as compared to the smooth tuner. In particular, our simulations indicate that the threaded tuner is equivalent to a smooth tuner of 2.2 mm in diameter. This effect may be justified by the fact that the threaded tuning element (a screw) has, indeed, a smaller total volume with respect to a smooth rod of the same diameter and length. As a result, the phase shift introduced by the screw is lower.

Next, we performed the same measurement, using this time SS tuners. Fig. 4 shows the result obtained. As expected, the SS tuners give the same results as the aluminum tuners.

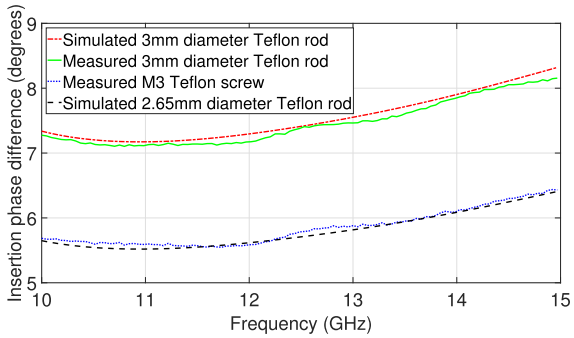

Fig. 5. Teflon tuners. Top: smooth rod and bottom: threaded. The simulated result have been obtained with CST design studio.

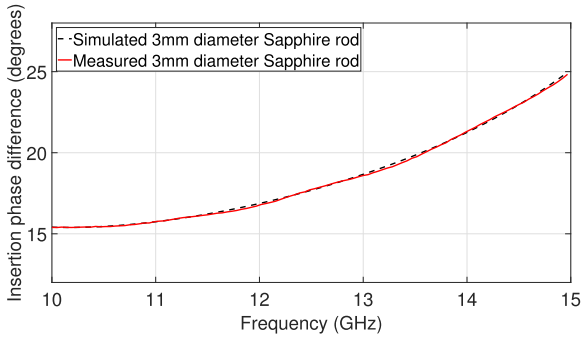

Fig. 6. Sapphire tuner. The simulated result have been obtained with CST design studio.

The next result has been obtained with the Teflon tuners (see Fig. 5). In this case, the tuners are allowed to penetrate until the lower surface of the waveguide (9.525 mm). As we can see, the effective diameter of the Teflon screw is now 2.65 mm.

The last result that we show is the measurement of the phase difference introduced by a smooth Sapphire rod of 3 mm in diameter (see Fig. 6), penetrating 4 mm.

It is important to note that the Sapphire rod has two values of dielectric constant, depending on the direction of energy propagation. If the energy propagates along the axis of the cylinder, the value is $\epsilon_r = 11.5$. If the energy propagates in a direction that is orthogonal to the axis of the cylinder, the value is $\epsilon_r = 9.3$. In our case, therefore, we have used $\epsilon_r = 9.3$.

III. Passive Intermodulation Experiment

The generation of PIM products in high-power microwave components in general, and waveguide filters in particular, is an issue that has been known for quite some time [28], [42]. In physical terms, PIM is a nonlinear effect due to several reasons. Among the most important we find the metal-to-metal contacts. Under certain conditions, a metal-to-metal contact can have a nonlinear transfer function, so that an RF current crossing the contact line can result in PIM generation [29], [43]. Intermodulation products can have a very serious degrading effect at the system level, so that particular care must be taken to avoid the generation of PIM (see for instance [44]). It is therefore a standard industry practice to measure the PIM generation characteristics of microwave hardware with dedicated measurement benches [45].

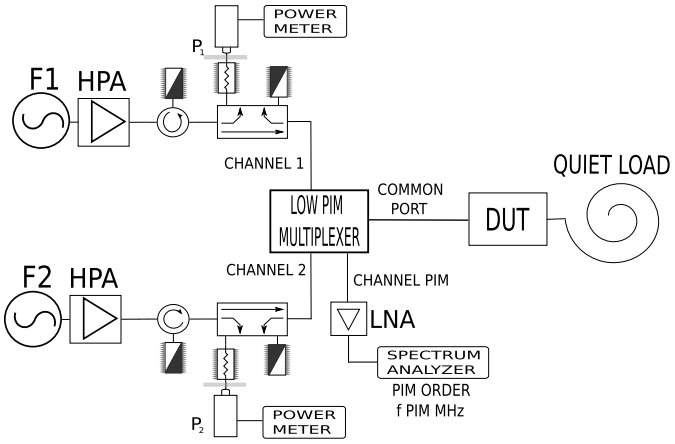

Fig. 7. PIM test bed circuit description.

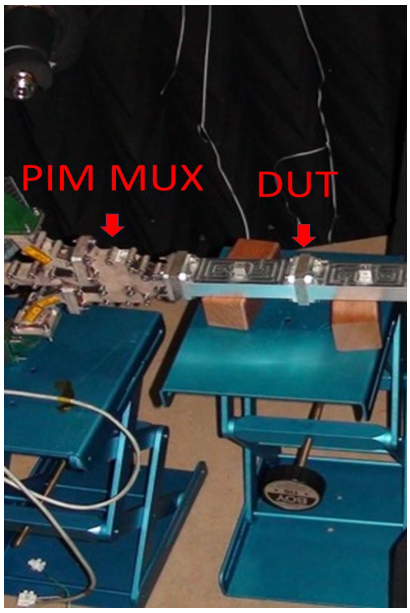

Fig. 8. PIM test bed configuration including the DUT. The PIM MUX and the DUT are clearly identified.

In the context of this article, it is therefore important to investigate the PIM behavior of the various tuning elements described in Section II. A PIM measurement was therefore carried out with the DUTs shown in Fig. 1, and with the following measurement parameters.

1) *Channel 1:* $f_1 = 11\,468$ MHz, Power 10-W continuous wave (CW).
2) *Channel 2:* $f_2 = 12\,735$ MHz, Power 10-W CW.
3) *Channel PIM Order 3:* $2f_2 - f_1 = 14\,002$ MHz.

Although the PIM measurement parameters are normally chosen with respect to a specific application, in our case the choice of power levels and frequencies has been dictated by the availability of the measurement setup in our laboratory. As a consequence, the parameters chosen for the PIM measurement are not specifically linked to a particular application. They are, however, fully appropriate to evaluate the PIM behavior of the tuning elements being investigated. Fig. 7 shows the circuit description of the PIM test setup we have used. Fig. 8 shows the DUT within the measurement setup used to obtain the experimental PIM data.

The setup that we have chosen for this measurement is a conducted backward PIM test setup working in *Ku*-band. The core of the setup is a low PIM multiplexer manufactured in clam–shell technology, and silver plated [46]. The outstanding PIM performance of this specific multiplexer (about 200 dBc between carriers and PIM) is described in [45, Table IV]. In this context, however, it is important to recall that the actual noise floor of each specific PIM test bed depends very strongly on the type of flanges used to connect the DUT to the test bed [43], and the DUT used in this article was built with standard WR75 flanges and not with low PIM flanges.

Before performing the actual PIM measurements, we have first measured the residual PIM noise floor of our test setup. This measurement has been performed without any tuning elements in the DUT, and with two carriers of 10 W each. The value we measured is -110 dBm, as reported in Table I (Blank). This is equivalent to 150 dBc between transmission carriers and PIM. This is indeed the standard situation that is applicable to nonsilver-plated waveguide components. The measured noise level is therefore well below the one requested for conventional PIM measurements, and is very close to the one of state-of-the-art units [47], [48]. As a consequence, the performance of the test bed we used is fully adequate for our purposes, since the measurement discussed in this article are aimed at measuring relative PIM levels and not absolute levels.

TABLE I
PIM RESULTS SUMMARY

Material	Min. Pen.	PIM (dBm)	Max. Pen.	PIM (dBm)
Blank	N.A.	N.A.	N.A.	-110
Sapphire	0.5	-111	4	-111
Teflon	N.A.	N.A.	9.525	-110
SS Screw	1.0	-98	2	-70
Alu. Rod (1)	0.5	-109	2	-70
Alu. Rod (2)	0.5	-110	2	-110
Alu. Screw	1	-109	2	-110

It is important to note at this point that, although the focus of this article is on reconfigurable filters, the DUT selected for the PIM measurement is a straight piece of waveguide instead of a resonator (or a filter). The reason for this choice is that we wanted to focus only on the PIM behavior of the tuning element. Using a filter with tuning screws as a DUT, would have required a more complex structure with more mating surfaces. The DUTs in Fig. 1, on the other hand, are built using spark erosion on a single piece of aluminum, thus reducing to a minimum the required mating surfaces, and therefore drastically reducing any possible source of PIM other than the tuning elements. A summary of the results obtained for all the PIM measurements performed is shown in Table I.

The first PIM measurement was carried out with the Sapphire rod, obtaining the results shown in the second row of data in Table I. In Table I, for the sake of space, we only show the minimum penetration for which PIM generation was detected, and the measured PIM level at the maximum penetration. From

the data, we can see that the Sapphire tuning rod does not generate PIM above the residual PIM level of the test facility.

We the carried out the measurement with the Teflon screw inserted completely inside the DUT (that is, with a penetration of 9.525 mm). The results are shown in the third row of Table I. The PIM produced by Teflon is again below the reference PIM level (blank scenario).

The next material we measured is SS. In this case, the tuning screw was properly locked with a locking nut. The results obtained are shown again in Table I (fourth row). Form our measurements, it appears that when the SS screw penetrates over 1.0 mm, it does generate strong PIM. This result was, indeed, expected, since the contact between the SS screw and the aluminum body of the DUT introduces a nonlinearity in the microwave current flow.

The next measurement was carried out with a smooth aluminum rod (see Table I, fifth and sixth rows). In the first measurement [fifth row Alu. Rod. (1)], the rod was blocked with a lateral (orthogonal) screw (as described in the caption of Fig. 1). From the measurement results, it is evident that when the aluminum rod penetrates more than 0.5 mm, it also generates PIM. This is indeed a surprising result since theoretically, a tuning element made of the same metal as the body of the device should not generate PIM. Upon closer examination of the DUT, we then discovered that the lateral fixing screw we used was an SS screw. The appearance of PIM, in this case, is therefore due to a nonlinearity caused by the lateral SS screw used for blocking the tuning rod. The experiment was repeated using a Teflon screw to block the aluminum rod and, as expected, no PIM was detected (see Table I, sixth row).

The last measurement that we carried out is for the aluminum screw locked in place with a nut made of SS (see Table I, seventh row). When the aluminum screw is locked by a nut, even if the nut is made of another metal, the tension produced generates a homogeneous metal-to-metal contact between the screw and the body of the DUT (both the screw and the DUT are made of the same metal), so that the screw does not generate PIM above the residual PIM level of the test facility.

One final important remark concerning the PIM behavior of both metallic and dielectric tuners is that what we have studied is their PIM behavior in a piece of straight waveguide. As already mentioned, this has been done to focus our research only on the isolated tuning elements. The actual PIM level produced by a tuning element embedded in a filter, however, may depend also on other aspects like the filter bandwidth, specific center frequency, workmanship, and other manufacturing details of the filter itself. This is why it is always recommended to perform dedicated PIM measurements for each specific device of interest.

The value of our contribution, in the context of this article, is indeed in the confirmation that dielectric tuners by themselves do not produce PIM, and that we need to pay close attention to the manufacturing details, because PIM can be generated also by elements, like the lateral fixing screw, that are not strictly inside the filter resonators or apertures.

IV. Tuning Range Investigation

A. From Phase Shift to Tuning Range

Before investigating the achievable tuning range with a complete filter, we now discuss the relation between phase shift and the resonant frequency of a short-circuited, half-wavelength long resonator in rectangular waveguide that contains a tuning element. Naturally, we assume in the remainder of this section that the resonant frequency of interest is within the frequency range investigated in Section II for the phase shift.

The basic well-known resonant condition for such a structure without any tuning element is as follows:

$$\beta l_{\text{res}} = \pi \tag{1}$$

where l_{res} is the length of the resonator. From (1), we can easily obtain an expression for the resonance frequency f_{res} of the TE_{101} mode, namely,

$$f_{\text{res}} = \frac{1}{2\sqrt{\epsilon_0 \mu_0}} \sqrt{1/a_{\text{res}}^2 + 1/l_{\text{res}}^2} \tag{2}$$

where a_{res} is the width of the rectangular waveguide.

If we now introduce in the resonator a tuning element that introduces an additional phase shift $\Delta\phi_{\text{res}}$ (in degrees), we can write

$$\beta l_{\text{res}}^{(t)} + \Delta\phi_{\text{res}} \frac{\pi}{180} = \pi \tag{3}$$

where $l_{\text{res}}^{(t)}$ is the actual physical length of the resonator with the tuning element. From (3), we can now easily obtain the following expression:

$$l_{\text{res}}^{(t)} = \frac{\left(1 - \frac{\Delta\phi_{\text{res}}}{180}\right)}{\sqrt{\left(2 f_{\min}^{(t)} \sqrt{\epsilon_0 \mu_0}\right)^2 - \left(1/a_{\text{res}}^2\right)}} \tag{4}$$

where $l_{\text{res}}^{(t)}$ is the length of the resonator that is required to produce a resonance at $f_{\min}^{(t)}$ when the tuner introduces the maximum phase shift equal to $\Delta\phi_{\text{res}}$. It is important to note, at this point, that the minimum resonant frequency $f_{\min}^{(t)}$ is indeed obtained when the tuner is fully inserted, thus providing the corresponding phase shift

$$\Delta\phi_{\text{res}} = 2\Delta\phi \tag{5}$$

where $\Delta\phi$ is the value given by the phase shift curves in Section II.

It is now important to note that the presence of the factor 2 in (5) can be easily explained in terms of the well-known perturbation theory. In fact, according to that theory, the change in frequency of a resonator, and therefore the phase shift, depends on the stored energy in the volume of the perturbation introduced in the cavity. Now, in a cavity the total field is the sum of two identical waves traveling in opposite directions. However, in an adapted waveguide, there is only one wave. As a consequence, the total phase shift in a cavity is twice the phase shift induced by the same perturbation in a straight waveguide.

With simple calculations, we are now able to derive from (4) an expression for the minimum resonant frequency $f_{\min}^{(t)}$

TABLE II
RECONFIGURATION RANGE COMPARISON USING TEFLON AND SAPPHIRE TUNERS

$\Delta\phi_{res}@f_{min}$ (Sapphire)	length of resonator (l_{res}) in mm	f_{min}(simulated) GHz	$f_{min}^{(t)}$(calculated) GHz	frequency error in %	f_{max}(simulated) GHz	$f_{max}^{(t)}$(calculated) GHz	frequency error in %
31.488	16.098	11.008	11.005	0.02725	12.1909	12.199	0.0664
35.3702	12.45207	12.503	12.477	0.207950	14.3814	14.391	0.0667
39.692	10.7289	13.502	13.445	0.4221	16.0346	16.046	0.071
$\Delta\phi_{res}@f_{min}$ (Teflon)	length of resonator (l_{res}) in mm	f_{min}(simulated) GHz	$f_{min}^{(t)}$(calculated) GHz	frequency error in %	f_{max}(simulated) GHz	$f_{max}^{(t)}$(calculated) GHz	frequency error in %
14.346	17.84989	11.0	11.0375	0.3409	11.508	11.516	0.0695
14.8234	14.09525	12.5	12.544	0.352	13.2291	13.238	0.0672
15.43	12.43883	13.5	13.548	0.355	14.3921	14.402	0.06878

that we obtain having the tuner fully inserted in a resonator of length $l_{\text{res}}^{(t)}$, namely,

$$f_{\text{min}}^{(t)} = \frac{1}{2\sqrt{\epsilon_0\mu_0}}\sqrt{1/a_{\text{res}}^2 + (1-\Delta\phi_{\text{res}}/180)^2/\left(l_{\text{res}}^{(t)}\right)^2}. \quad (6)$$

To continue, we now note that once the physical length of the resonator is fixed, we can easily compute, using (2), the maximum resonant frequency $f_{\text{max}}^{(t)}$ that is obtained when the tuner is removed from the resonator, namely,

$$f_{\text{max}}^{(t)} = \frac{1}{2\sqrt{\epsilon_0\mu_0}}\sqrt{1/a_{\text{res}}^2 + 1/\left(l_{\text{res}}^{(t)}\right)^2}. \quad (7)$$

We can now easily obtain from (6) and (7) the following expression:

$$\left(f_{\text{max}}^{(t)}\right)^2 - \left(f_{\text{min}}^{(t)}\right)^2 = \frac{1}{\left(2l_{\text{res}}^{(t)}\right)^2\epsilon_0\mu_0}\frac{\Delta\phi_{\text{res}}}{180}\left(2-\frac{\Delta\phi_{\text{res}}}{180}\right) \quad (8)$$

where we can see that the tuning range is indeed simply related to the maximum phase shift introduced by the tuner, and the physical length of the resonator $l_{\text{res}}^{(t)}$.

To use the expressions just derived, we must first decide which tuning element we are going to use among the ones investigated. We then decide the minimum resonant frequency $f_{\text{min}}^{(t)}$ that we need for the given application, and we obtain from the phase shift curves the corresponding value of $\Delta\phi$. We can now compute with (4) and (5) the required resonator length $l_{\text{res}}^{(t)}$. Finally, we can compute the achievable tuning range using (8).

Next, to further investigate the validity of the equations we just derived, we have conducted two experiments using the phase shift results shown in Figs. 5 (teflon) and 6 (sapphire). The experiments consisted in simulating a WR75 cavity with dielectric tuners using CST studio. The results obtained are given in Table II, where the values of f_{min} and f_{max} obtained with CST are compared with the values calculated using (6) and (7). In addition, the variation in resonant frequency as a function of the tuner penetrations are shown in Figs. 9 and 10 for Sapphire and Teflon, respectively. As we can see in Table II, the simple equations that we have derived are indeed very accurate.

Naturally, if the tuning range that is finally obtained is not enough for the application under consideration, we must increase the diameter of the tuner and/or the value of the dielectric constant.

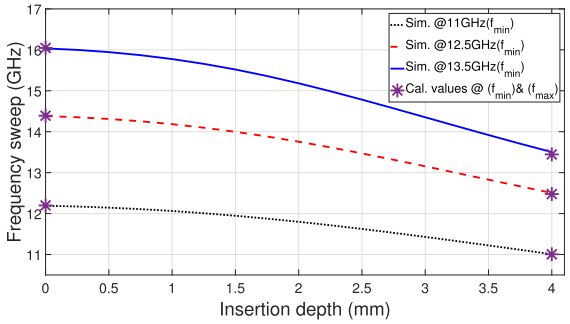

Fig. 9. Comparative graph of simulated and calculated resonant frequency sweep for sapphire tuner.

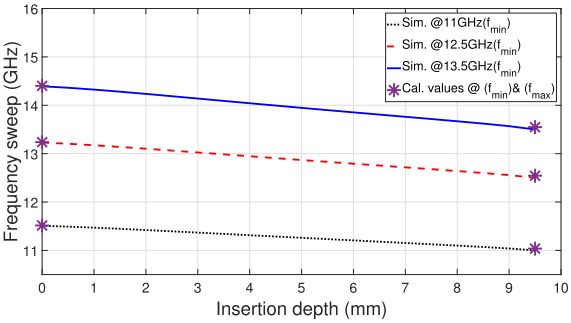

Fig. 10. Comparative graph of simulated and calculated resonant frequency sweep for teflon tuner.

Finally, it is important to note that, the evaluation of the effects of a dielectric tuner on a cavity could have also been obtained performing experiments directly using a cavity coupled to an input and an output waveguide (that is a one-pole filter). However, using a one-pole filter we would have needed to consider two additional effects. The first is that there is always an interaction between tuning elements and coupling apertures, and this interaction is eliminated using only the phase shift measurement. The second is that as the frequency is lowered, the bandwidth of a resonator with fixed input and output couplings decreases. As a consequence, to keep the bandwidth constant, we would have needed different resonators or a resonator with tunable couplings. With the procedure we have described, on the other hand, a single measurement (or simulation) can give the tuning behavior of a given tuner in the complete frequency range of interest.

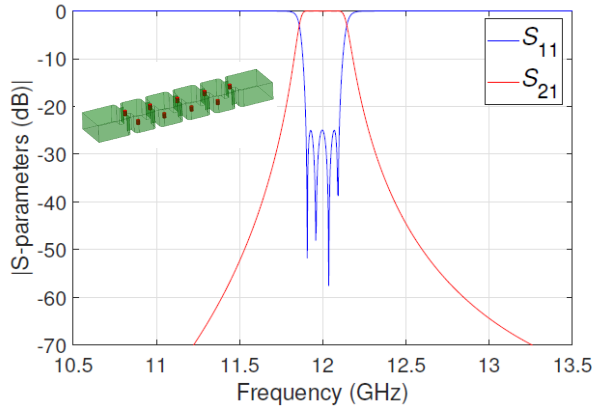

Fig. 11. Basic four-pole rectangular waveguide inductive filter structure and performance.

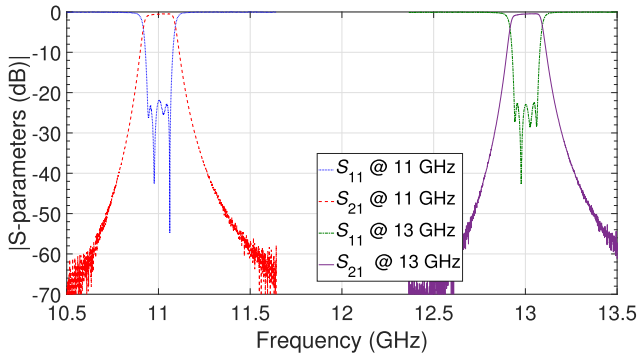

Fig. 12. Measured response of the tunable (metallic tuners) silver-plated filter (11 GHz: IL 0.44 dB, $Q = 2183$, 13 GHz: IL 0.40 dB $Q = 2838$).

B. Reference Filter Structure

The next step in our investigation has been to define a reference filter structure, namely, a standard, inductively coupled, rectangular waveguide filter, as shown in Fig. 11 for the performance and the basic structure (insert), with the following electrical characteristics.

1) Center frequency $f_0 = 12$ GHz.
2) Bandwidth BW = 200 MHz (1.7%).
3) Return losses: RL = 25 dB.

The physical dimensions of the reference filter are given in Table III, together with the dimensions of all other filters discussed in this article. Note that the reference filter structure was already discussed in [36], however, this information is repeated here for the sake of completeness.

The filter is manufactured in silver-plated aluminum, with 2-mm curvature radius in all concave corners. Fig. 12 and Table IV show the measured performance and the related metallic tuner penetrations, respectively. The insertion losses achieved are 0.44 (11) and 0.40 dB (13 GHz). Using this information, we have estimated the quality factors of the resonators using the method described in [2]. The values obtained are $Q = 2183$ (11 GHz) and $Q = 2838$ (13 GHz).

C. Experimental Investigation

An initial tuning range estimation was performed prior to the experimental verification. The initial results obtained using Teflon tuning rods have been already reported in [36]. However, for the sake of completeness, we report here a summary (see Table V) of the results obtained in [36].

As we can see, a very limited tuning range can be obtained using only 2-mm tuning rods, while a tuning range of about 570 MHz can be achieved using 2-mm rods in the apertures, and 4-mm rods in the cavities.

Next, we discuss the experimental results obtained with Sapphire rods ($\epsilon_r = 9.3$ for propagation perpendicular to the cylinder axis) of different diameters. In the first measurement

TABLE III
FILTERS DIMENSIONS (mm)

Filter element	Fig. 11	Fig. 15	Fig. 17
Waveguide	WR75	WR90	WR90
Radius of corners	2.0	2.0	2.0
Iris thickness	2.5	4.0	4.0
I/O aperture	8.529	12.630	12.698
Second aperture	5.339	8.934	9.011
Central aperture	4.959	8.313	8.391
First cavity	12.188	14.743	14.742
Second cavity	13.424	16.979	16.981

TABLE IV
THEORETICAL METALLIC TUNING SCREWS PENETRATIONS (mm)

Filter element	11 GHz	12 GHz	13 GHz
I/O aperture	3.61	2.73	0.49
First cavity	3.41	2.48	0.47
Second aperture	3.85	2.89	0.50
Second cavity	3.66	2.69	0.49
Centered aperture	3.76	2.70	0.50

TABLE V
TUNING RANGE SUMMARY USING TEFLON AND SAPPHIRE
($F_{\max}$ 13 GHz, BW 200 MHz)

Teflon Tuners	ΔF_0 MHz	IL ($dB@F_{max}$)	RL (dB)
2mm (all)	-128	0.61	≤ 18
2-4mm (coup-res)	-575	0.65	≤ 18
Sapphire Tuners	ΔF_0 MHz	IL ($dB@F_{max}; F_{min}$)	RL (dB)
3mm	-500	0.65;0.85	≤ 18
4mm	-500	0.6;0.8	≤ 18

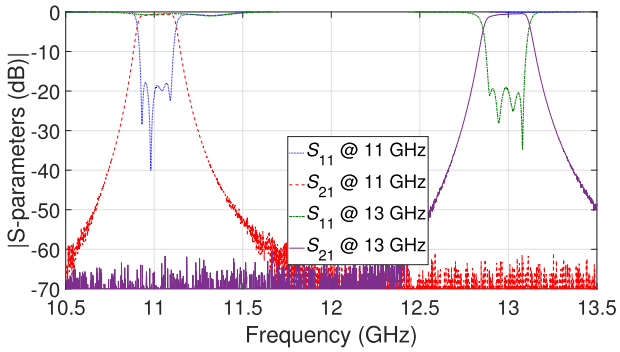

Fig. 13. High-end (right curve, IL 0.61 dB, $Q = 1861$) and low-end (left curve, IL 0.74 dB, $Q = 1298$) performance with nonsilver-plated WR75-based filter with 2-mm Sapphire rods.

TABLE VI
THEORETICAL 2-mm SAPPHIRE TUNING RODS PENETRATIONS (mm)

Filter element	11 GHz	13 GHz
I/O aperture	6.00	1.50
First cavity	8.20	1.0
Second aperture	6.00	1.50
Second cavity	8.20	1.0
Central aperture	6.00	1.50

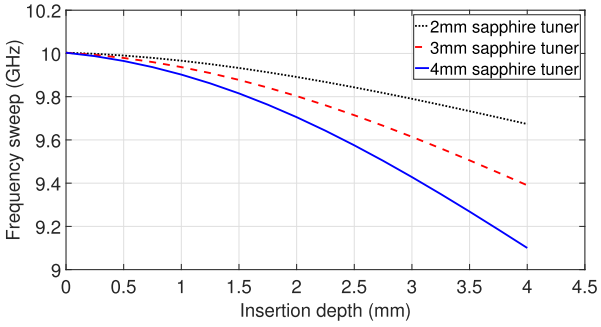

Fig. 14. WR90 resonator: Tuning range with 2-, 3-, and 4-mm tuners.

we have performed, we have used Sapphire rods of 2 mm as tuning elements. In Fig. 13, we show the tuned filter responses at the minimum (low-end) and at the maximum (high-end) frequencies of the achievable tuning range that can be obtained with Sapphire. As we can see, with 2-mm Sapphire rods, we have obtained almost the same tuning range given by the silver-plated aluminum rods (as reported in [36]). The insertion loss obtained in this case is 0.74 dB at the lower center frequency, and 0.61 dB at the higher center frequency.

It is important to note that the Sapphire tuning rods are practically fully inserted at the low-end performance (8.2 mm theoretically from previous simulations, as we can see in Table VI). Also in this case, we have a higher physical movement of the tuning element with respect to the silver-plated aluminum case. Again, this is indeed an advantage since the filter response is less sensitive to small variations in the tuning element penetration.

Finally, we have performed two more measurements using as tuning elements Sapphire rods of 3 and 4 mm. The results obtained are summarized in Table V. As we can see from Table V, a tuning range of only 500 MHz has been obtained in both cases. Further investigation indicates that the reduced tuning range is due to the direct interaction that takes place between the larger tuning elements. This result is relevant, in our opinion, because it indicates that, for each dielectric material and specific filter geometry, there will be an optimal choice for the diameter of the tuning rods to achieve the maximum tuning range. For our WR75 filter, it turns out that the 2-mm diameter Sapphire tuner produces the maximum tuning range among all three experiments, as shown in Fig. 13.

To conclude this part of our investigation, we have next performed a number of simulations (CST) using a WR90 resonator and sapphire tuners of various diameters, as shown in Fig. 14. As expected, the tuning range increases when increasing the diameter of the tuner.

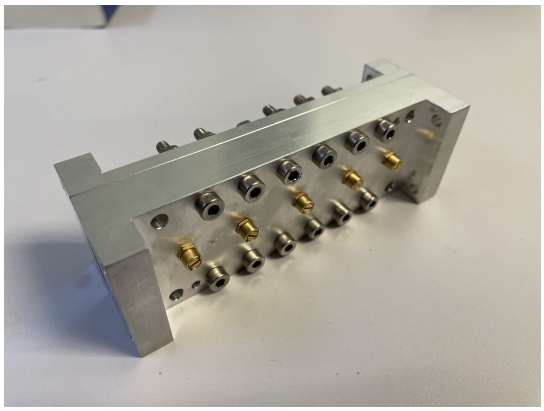

Fig. 15. Manufactured WR90 standard filter with metallic tuners.

TABLE VII
THEORETICAL METALLIC TUNING SCREWS PENETRATIONS (mm)

Filter element	8.3 GHz	9.3 GHz	10 GHz
I/O aperture	4.358	2.873	1.0
First cavity	4.006	2.745	1.0
Second aperture	4.664	3.151	1.0
Second cavity	4.469	3.009	1.0
Central aperture	4.688	3.067	1.0

D. WR90 Based Filter Structure

To proceed with our investigation, we now discuss the results obtained with a filter based on a WR90 waveguide. Both metallic and Sapphire tuners will be used. This investigation has been performed to verify the need for a different dielectric tuner diameter when using different waveguide sizes. As in the case of the WR75, we have used as a reference an inductively coupled rectangular waveguide filter similar to the one shown in the insert of Fig. 11. The only difference is that now we use a WR90 instead of a WR75 waveguide. The thickness of the inductive window has been set at 4 mm. The reference filter is designed with all tuners penetrating 1 mm inside the filter. The specifications of the WR90 filter are as follows.

1) Center frequency $f_0 = 10.0$ GHz.
2) Bandwidth BW $= 300$ MHz (3%).
3) Return losses: RL > 25 dB.

1) Experiment With Metallic Tuner: The next step is to carry out the tuning experiment in the WR90 waveguide filter using the metallic tuner. A standard commercial tuner (205-0901-100) manufactured by Tronser GmbH of 3.2 mm of diameter has been used to tune the filter. The final assembly is shown in Fig. 15. Table VII shows the theoretical values of the screw penetrations that are required to obtain the desired bandpass response at different center frequencies. The dimensions of the basic filter structure are given in Table III.

The measured response of three separate tuned states (channels) is shown in Fig. 16 as compared to simulations. As we

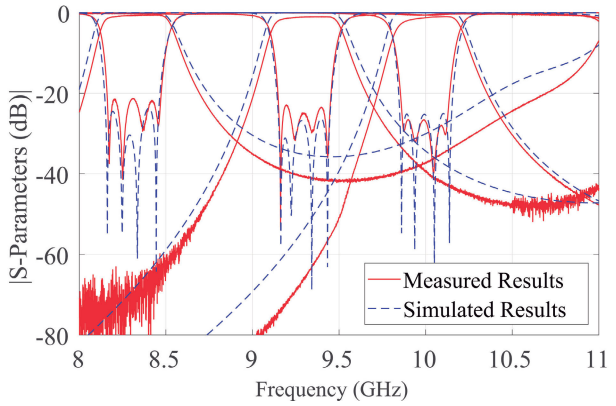

Fig. 16. High-end (right curve, IL 1.07 dB, $Q = 541$), center (IL 1.05 dB, $Q = 515$), and low-end (left curve, IL 0.99 dB, $Q = 489$) performance of nonsilver-plated WR90-based filter with 3-mm metallic tuners.

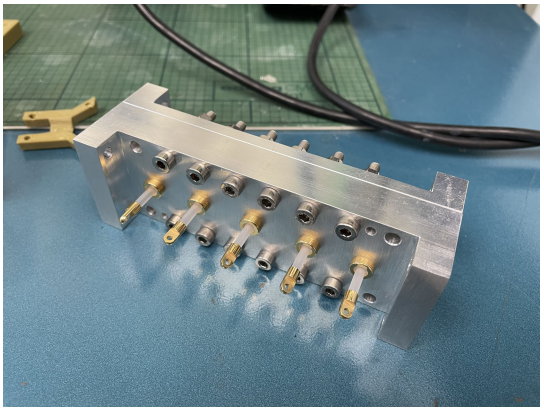

Fig. 17. Manufactured WR90 standard filter with customized dielectric tuners.

can see, starting from 10 GHz, the filter has been tuned down to a center frequency of 8.3 GHz, while maintaining a constant bandwidth. This is indeed the maximum tuning range achievable due to the appearance of a spurious response at 11 GHz. For each tuned state, the measured insertion losses and the estimated Q factor are 0.99 dB ($Q = 489$) at the lower end, and 1.07 dB ($Q = 541$), at the high end, as indicated in the caption of Fig. 16.

2) Experiment With Dielectric Tuner: In this section, we discuss the experimental results carried out with the Sapphire rods ($\epsilon_r = 9.3$ for propagation perpendicular to the cylinder axis) of 3 mm in diameter. To this end, we designed a filter in a WR90 waveguide incorporating the Sapphire rod as the tuning element, thus obtaining a new set of dimensions for the basic structure (see Table III). A customized tuner manufactured by Tronser GmbH has been used in this study [49]. The final assembled structure is shown in Fig. 17.

Furthermore, this study has been carried out using computer controlled linear actuators. It is important to note that, for this demonstrator, we have used low-cost commercially available piezoelectric linear actuators. Each dielectric tuner is connected to an independently controlled linear actuator, as shown in Fig. 18. The position of the actuators is then con-

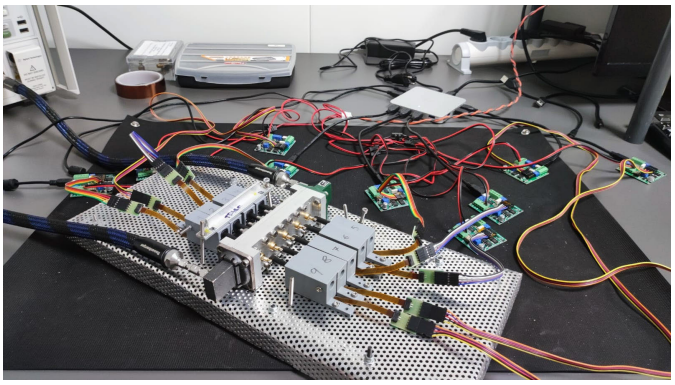

Fig. 18. Computer controlled setup for remote tuning using dielectric tuners, and linear actuators Acutonix PQ12-P (100:1). The actuators have the following main characteristics: positional repeatability = ±0.1 mm, mechanical backlash = ±0.25 mm, and stroke displacement = 20 mm. The complete set of specifications can be found at https://www.actuonix.com/pq12-100-6-p.

TABLE VIII
THEORETICAL DIELECTRIC TUNER PENETRATIONS (mm)

Filter element	8.3 GHz	9.25 GHz	10 GHz
I/O aperture	7.8551	4.261	1.0
First cavity	6.838	3.922	1.0
Second aperture	9.506	5.078	1.0
Second cavity	8.002	4.453	1.0
Central aperture	9.592	5.074	1.0

trolled using a standard personal computer (PC). The tuning experiment is initiated by setting the tuners to the theoretical penetrations given in Table VIII. Furthermore, the response for each filter center frequency is fine tuned to obtain the desired response. The final experimental penetration values are shown in Table IX.

It is important to note that in Table IX we give only percentage penetration values and not millimeter values. This has been done because the actual penetration in millimeters depends, in addition to the effect of the dielectric tuner, also on the mechanical inaccuracies due to the manufacturing process used to make the filter. The relevant information in this context is whether or not the tuners can provide the required tuning range. This is indeed fully demonstrated by the data provided in Table IX.

In Fig. 19, we can see the tuned response at three channels covering the complete tuning range (high end, center channel, and low end). The simulated response (in dashed blue) is shown in the same graph. The measured insertion loss is 0.58 dB ($Q = 833$) at the lower end, and 0.69 dB ($Q = 848$) at the higher end of the tuning range. As we can see, the dielectric tuners have achieved almost the same tuning range as the metallic tuners, but with a better-quality factor.

To further demonstrate the possibility of remote tuning, we have changed the tuning states of the dielectric tuners from one channel to another for five times for each channel using the penetrations given in Table IX. The measured results obtained are shown in Fig. 20 showing a very good level of repeatability. It is important to note in this context that the objective of this

TABLE IX
EXPERIMENTAL DIELECTRIC TUNER PENETRATIONS (50% CORRESPONDS TO 1.0 mm)

Frequency (GHz)	Motor 1	Motor 2	Motor 3	Motor 4	Motor 5	Motor 6	Motor 7	Motor 8	Motor 9
10 GHz	50%	50%	50%	50%	50%	50%	50%	50%	50%
9.25 GHz	67.4%	77.7%	76%	76.4%	70.2%	75.2%	76.7%	80.1%	70.2%
8.25 GHz	84.3%	93.8%	93.0%	90.9%	85.2%	91.2%	91.5%	91.2%	85.9%

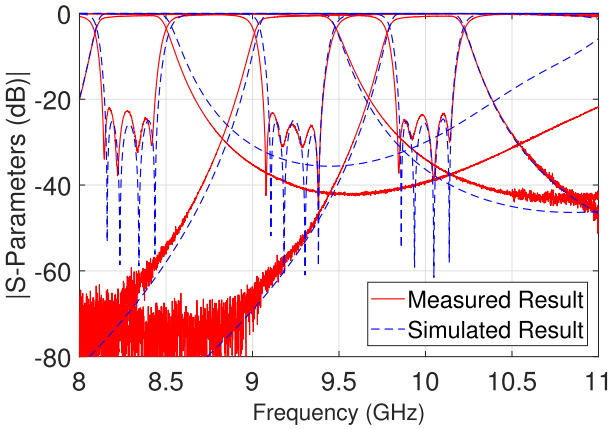

Fig. 19. Three channel performance of nonsilver-plated WR90-based filter with 3-mm Sapphire rods. High-end (right curve, IL 0.69 dB, $Q = 848$), center (IL 0.64 dB, $Q = 843$), and low-end (left curve, IL 0.58 dB, $Q = 833$).

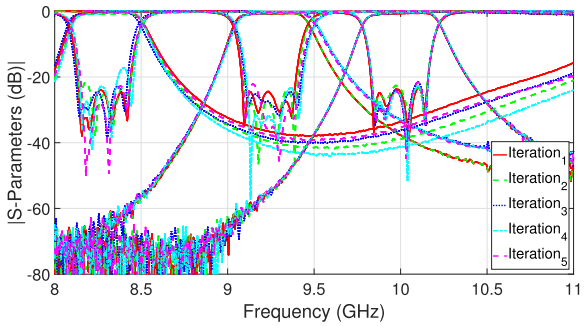

Fig. 20. Repetitive experiment of remote tuning with 3-mm Sapphire rods.

article is to provide a proof of concept. Finally, it is interesting to note that, even though we have used inexpensive actuators (see Fig. 18), the variation between successive experiments has been relatively small. The total error in the center frequency is approximately ±5 MHz, and the variation in bandwidth is approximately ±10 MHz; the minimum and maximum value of insertion losses at the center frequency are, 0.518 and 0.79 dB, respectively. The theoretical value of return loss is 25 dB; however, the minimum is 18 dB, and the return loss level is nearly constant with an uncertainty of 2–3 dB in all five attempts. A much better result can certainly be obtained with a more carefully designed setup.

V. RECONFIGURING THE FILTER BANDWIDTH

We now discuss an additional set of results, namely, the possibility of reconfiguring the filter bandwidth in addition to the filter center frequency. This is indeed possible since with our structure we can tune individually all couplings and all resonators.

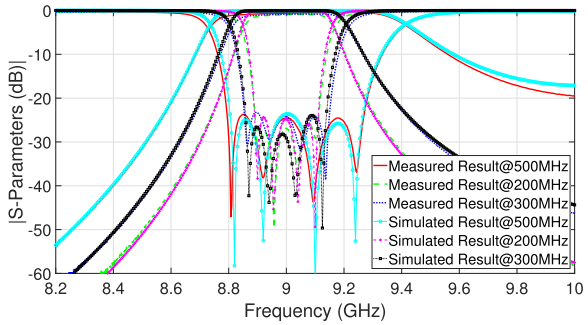

Fig. 21. Filter structure tuned for three different bandwidths. Both simulated and measured results are shown.

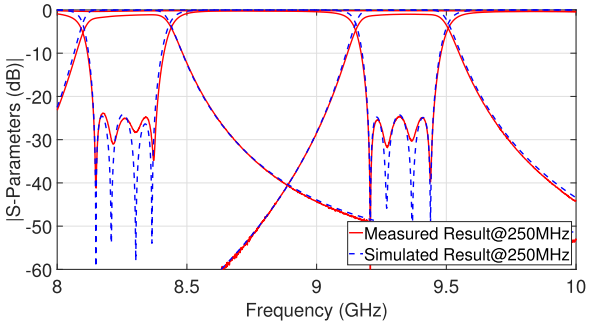

Fig. 22. Center frequency tuning range for 250-MHz bandwidth. Both simulated and measured results are shown.

To demonstrate this feature, we have started by tuning the WR90 filter in the center of the tuning range (see Fig. 19). We have then increased progressively the filter bandwidth till the maximum allowed by the structure. We have then tuned again the filter but this time for the minimum bandwidth. Fig. 21 shows the comparison between simulated and measured results for the three cases, namely, narrow, nominal, and wider bandwidth. As we can see in Fig. 21, we have been able to reconfigure the filter from a minimum bandwidth of 200 MHz, to a maximum of 500 MHz, while maintaining an equiripple response. It is important to note that any other value of bandwidth between 200 and 500 MHz can also be easily obtained.

We have next explored the maximum tuning range that the structure allows while maintaining the same equiripple bandwidth of 250 MHz. The results obtained are shown in Fig. 22. As we can see from Fig. 22, we have been able to tune the filter from 9.32 down to 8.27 GHz.

The final set of results that we discuss is the possibility of tuning the filter center frequency with a wider bandwidth rather than with a reduced bandwidth. For this purpose, we have chosen a bandwidth of 400 MHz. The results obtained

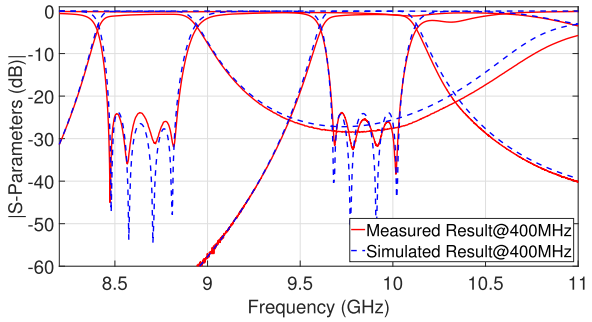

Fig. 23. Center frequency tuning range for 400-MHz bandwidth. Both simulated and measured results are shown.

are shown in Fig. 23. As we can see from Fig. 23, we have been able to tune the filter from 9.84 down to 8.65 GHz.

VI. Comparative Discussion

The results described in this contribution indeed show that dielectric tuning elements offer several advantages with respect to metallic tuning elements, as follows.

1) The insertion loss introduced by dielectric tuning elements is of the same order of magnitude as the one introduced by metallic tuning elements.
2) Dielectric tuners do not require good electric contact with the body of the filter.
3) For the same frequency tuning range, dielectric tuners penetrate significantly more inside the filter than metallic tuners.
4) The relatively large movement needed by dielectric tuners makes it possible to obtain good repeatability even with commercial low-cost, computer-controlled linear actuators.

The last feature is indeed very interesting for possible remotely tuned implementations. In particular, taking for example the variation in penetration of the tuning element in the central aperture in Tables VII (3.688 mm) and VIII (8.592 mm), we can see that the sensitivity of the metallic tuner is about 2 μm/MHz, while the sensitivity of the dielectric tuner is about 5 μm/MHz. This difference makes it indeed possible to use low accuracy linear actuators directly connected to the dielectric tuners. If we were to use the same actuators but with metallic tuners, we would need to add a mechanical component (a gear) to compensate for the reduced excursion. This, in turn, would result in a significantly more complex implementation. Furthermore, to use metallic tuners we need to ensure good electric contact between the tuner and the body of the filter. This, in turn, would add substantial mechanical complexity and reduce very significantly the life of the tuning system do to the inevitable wear of the metal-to-metal contact. This tribology aspect is greatly simplified in the implementation shown in Fig. 17, since the holders of the dielectric tuners are built with a thin Teflon sleeve between the dielectric and the inner metallic body of the tuner. These considerations, in our opinion, do confirm that dielectric tuners are more suitable than metallic tuners for remotely controlled tuning implementations.

Furthermore, it is important to note that the filters discussed in this article have a bandwidth of 1.7%, and 3%, for WR75 and WR90, respectively. However, if narrower (or larger) bandwidths are required, we simply need to select the proper dielectric constant and dielectric rod diameter to maintain the appropriate linear motion sensitivity. It is also important to note that, so far, we have investigated only the use of Teflon and Sapphire dielectrics. However, a large variety of potentially useful dielectrics is available in the market.

VII. Conclusion

In this article we have given a number of contributions to the state-of-the-art of inductive, reconfigurable filters in rectangular waveguide, as follows.

1) We have shown that the use of threaded or smooth tuning elements of the same diameter does not introduce the same phase shift for the same penetration depth. This has been shown for both dielectric and metallic tuning elements.
2) We have shown that dielectric tuning elements do not introduce significant PIM products. A series of dedicated measurements have been carried out with different dielectrics, and with different shapes, obtaining consistently the same results (PIM level below the PIM noise floor of the measurement setup).
3) We have demonstrated experimentally that using Sapphire tuning rods we can achieve essentially the same tuning range performance achievable with metallic tuning elements.
4) We have explored the tuning range using dielectric tuners of several sizes, thereby demonstrating that for each specific filter, a trade-off is required between the value of the dielectric constant, the diameter, and the maximum penetration of the tuner, to obtain the desired performance. In particular, we have shown that using dielectric rods of large diameter may actually decrease and not increase the tuning range.
5) Our investigation confirms that dielectric tuning elements need to penetrate far more inside the filter than metallic ones [50]. As a result, the use of dielectrics can introduce a very substantial reduction in the positional accuracy of the (dielectric) tuning element itself. This feature is indeed of very practical interest for the development of applications that require filter reconfiguration.
6) As a proof of concept of a remotely reconfigurable structure, we have shown the results obtained with a filter using a WR90 waveguide and Sapphire tuners of 3 mm in diameter. The position of the tuners has been controlled with low-cost commercial linear actuators coupled to a PC. The results obtained show a very good repeatability thereby fully validating the basic concept.
7) In addition, we have also demonstrated, both in terms of simulations and measurements that the structure that we propose can be reconfigured in terms of bandwidth in addition to center frequency.

Finally, it is important to note that, although the results presented in this article have been obtained using inductive filters in rectangular waveguide, they are applicable also to any other microwave filter (or device) that can use dielectric tuners in replacement of metallic tuning elements.

ACKNOWLEDGMENT

The authors would like to thank the European High RF Power Space Laboratory of the European Space Agency (ESA) and Val Space Consortium (VSC) for contributing with its installations—laboratory cofunded by the European Regional Development Fund—A way of making Europe.

REFERENCES

[1] M. Dishal, "Alignment and adjustment of synchronously tuned multiple-resonant-circuit filters," *Proc. IRE*, vol. 39, no. 11, pp. 1448–1455, Nov. 1951.

[2] G. L. Matthaei, L. Young, and E. M. Jones, *Microwave Filters, Impedance-matching Networks, and Coupling Structures*. Norwood, MA, USA: Artech House, 1980.

[3] J. B. Ness, "A unified approach to the design, measurement, and tuning of coupled-resonator filters," *IEEE Trans. Microw. Theory Techn.*, vol. 46, no. 4, pp. 343–351, Apr. 1998.

[4] G. Pepe, F. J. Gortz, and H. Chaloupka, "Sequential tuning of microwave filters using adaptive models and parameter extraction," *IEEE Trans. Microw. Theory Techn.*, vol. 53, no. 1, pp. 22–31, Jan. 2005.

[5] A. Morini, G. Venanzoni, M. Farina, and T. Rozzi, "Modified adaptive prototype inclusive of the external couplings for the design of coaxial filters," *IEEE Trans. Microw. Theory Techn.*, vol. 55, no. 9, pp. 1905–1911, Sep. 2007.

[6] A. E. Atia and A. E. Williams, "Narrow-bandpass waveguide filters," *IEEE Trans. Microw. Theory Techn.*, vol. MTT-20, no. 4, pp. 258–265, Apr. 1972.

[7] W. Meng and K. L. Wu, "Analytical diagnosis and tuning of narrowband multicoupled resonator filters," *IEEE Trans. Microw. Theory Techn.*, vol. 54, no. 10, pp. 3765–3771, Oct. 2006.

[8] S. Li, X. Fan, P. D. Laforge, and Q. S. Cheng, "Surrogate model-based space mapping in postfabrication bandpass filters' tuning," *IEEE Trans. Microw. Theory Techn.*, vol. 68, no. 6, pp. 2172–2182, Jun. 2020.

[9] B. F. Keats, R. R. Mansour, and R. B. Gorbet, "Design and testing of a thermally stable filter using bimetal compensation," in *IEEE MTT-S Int. Microw. Symp. Dig.*, Honolulu, HI, USA, Jun. 2007, pp. 1293–1296.

[10] Y. Wang and Q. Sui, "A new temperature compensation method of rectangular waveguide resonant cavities," in *Proc. Asia–Pacific Microw. Conf.*, Dec. 2005, p. 4.

[11] M. H. N. Potok, "Capacitive-iris-type mechanically tunable waveguide filters for the X-band," *Proc. IEE, B Electron. Commun. Eng.*, vol. 109, no. 48, Nov. 1962, pp. 505–510.

[12] M. A. Lamming, "Tunable irises for waveguide channel filters," in *Proc. ESA Workshop Adv. CAD Microw. Filters Passive Devices*, 1995, pp. 301–315.

[13] V. E. Boria, M. Guglielmi, and P. Arcioni, "Computer-aided design of inductively coupled rectangular waveguide filters including tuning elements," *Int. J. RF Microw. Comput.-Aided Eng.*, vol. 8, no. 3, pp. 226–235, May 1998.

[14] G. L. Matthaei, L. Young, and E. M. Jones, *Microwave Filters, Impedance-matching Networks, and Coupling Structures*. Norwood, MA, USA: Artech House, 1980.

[15] J. Ossorio, J. Vague, V. E. Boria, and M. Guglielmi, "Efficient implementation of the aggressive space mapping technique for microwave filter design," in *Proc. 47th Eur. Microw. Conf. (EuMC)*, Oct. 2017, pp. 644–647.

[16] V. K. Chaudhary, P. Verma, and U. Balaji, "Field theory based CAD of inductive iris waveguide filter," in *Proc. Asia–Pacific Microw. Conf. (APMC)*, Dec. 2001, pp. 318–321.

[17] M. Guglielmi, R. C. Molina, and A. A. Melcon, "Dual-mode circular waveguide filters without tuning screws," *IEEE Microw. Guided Wave Lett.*, vol. 2, no. 11, pp. 457–458, Nov. 1992.

[18] V. Boria, M. Guglielmi, and P. Arcioni, "Accurate CAD for dual mode filters in circular waveguide including tuning elements," in *IEEE MTT-S Int. Microw. Symp. Dig.*, vol. 3, Jun. 1997, pp. 1575–1578.

[19] W. Hauth, D. Schmitt, and M. Guglielmi, "Accurate modelling of narrow-band filters for satellite communications," in *IEEE MTT-S Int. Microw. Symp. Dig.*, Boston, MA, USA, vol. 3, Jun. 2000, pp. 1767–1770.

[20] V. Boria, G. Gerini, and M. Guglielmi, "Computer aided design of reentrant coaxial filters including coaxial excitation," in *IEEE MTT-S Int. Microw. Symp. Dig.*, Jun. 1999, pp. 1131–1134.

[21] H. Leblond et al., "When new needs for satellite payloads meet with new filters architecture and technologies," in *Proc. Eur. Microw. Conf. (EuMC)*, Sep. 2009, pp. 1712–1715.

[22] C. Arnold, J. Parlebas, and T. Zwick, "Center frequency and bandwidth tunable waveguide bandpass filter with transmission zeros," in *Proc. 10th Eur. Microw. Integr. Circuits Conf. (EuMIC)*, Sep. 2015, pp. 369–372.

[23] U. Rosenberg et al., "Reconfigurable doublet dual-mode cavity filter designs providing remote controlled center frequency and bandwidth re-allocation," in *Proc. 46th Eur. Microw. Conf.*, Oct. 2016, pp. 532–535.

[24] J. Ossorio, J. Vague, V. E. Boria, and M. Guglielmi, "Exploring the tuning range of channel filters for satellite applications using electromagnetic-based computer aided design tools," *IEEE Trans. Microw. Theory Techn.*, vol. 66, no. 2, pp. 717–725, Feb. 2018.

[25] G. Basavarajappa and R. R. Mansour, "Design methodology of a high-Q tunable coaxial filter and diplexer," *IEEE Trans. Microw. Theory Techn.*, vol. 67, no. 12, pp. 5005–5015, Dec. 2019.

[26] G. Basavarajappa and R. R. Mansour, "A tunable quarter-wavelength coaxial filter with constant absolute bandwidth using a single tuning element," *IEEE Microw. Wireless Compon. Lett.*, vol. 31, no. 6, pp. 658–661, Jun. 2021.

[27] K.-L. Wu, "An optimal circular-waveguide dual-mode filter without tuning screws," *IEEE Trans. Microw. Theory Techn.*, vol. 47, no. 3, pp. 271–276, Mar. 1999.

[28] M. Yu, "Power-handling capability for RF filters," *IEEE Microw. Mag.*, vol. 8, no. 5, pp. 88–97, Oct. 2007.

[29] R. J. Cameron, C. M. Kudsia, and R. R. Mansour, *Microwave Filters for Communication Systems: Fundamentals, Design, and Applications*, 2nd ed. Hoboken, NJ, USA: Wiley, 2018.

[30] A. I. Abunjaileh and I. C. Hunter, "Combline filter with tunable bandwidth and centre frequency," in *IEEE MTT-S Int. Microw. Symp. Dig.*, May 2010, pp. 1476–1479.

[31] J. C. Melgarejo, J. Ossorio, S. Cogollos, M. Guglielmi, V. E. Boria, and J. W. Bandler, "On space mapping techniques for microwave filter tuning," *IEEE Trans. Microw. Theory Techn.*, vol. 67, no. 12, pp. 4860–4870, Dec. 2019.

[32] S. B. Cohn, "Microwave bandpass filters containing high-Q dielectric resonators," *IEEE Trans. Microw. Theory Techn.*, vol. MTT-16, no. 4, pp. 218–227, Apr. 1968.

[33] S. J. Fiedziuszko et al., "Dielectric materials, devices, and circuits," *IEEE Trans. Microw. Theory Techn.*, vol. 50, no. 3, pp. 706–720, Mar. 2002.

[34] L. Accattino, G. Macchiarella, and G. Bertin, "Modelling techniques for dual-mode reconfigurable filters used in satellite applications," in *IEEE MTT-S Int. Microw. Symp. Dig.*, Jul. 2016, pp. 1–2.

[35] L. Accatino, G. Bertin, R. Vallauri, P. Macchiarella, P. Martin Iglesias, and F. Bartolomasi, "A dual-mode reconfigurable cavity with dielectric tuning screws," in *Proc. 3rd ESA Workshop Adv. Flexible Telecom. Payloads*, Mar. 2016, pp. 21–24.

[36] J. Ossorio, V. E. Boria, and M. Guglielmi, "Dielectric tuning screws for microwave filters applications," in *IEEE MTT-S Int. Microw. Symp. Dig.*, Jun. 2018, pp. 1253–1256.

[37] G. Macchiarella, L. Accatino, and A. Malagoli, "Design of Ka-band tunable filters in rectangular waveguide with constant bandwidth," in *Proc. IEEE Asia–Pacific Microw. Conf. (APMC)*, Dec. 2020, pp. 622–624.

[38] B. Yassini, M. Yu, D. Smith, and S. Kellett, "A Ku-band high-Q tunable filter with stable tuning response," *IEEE Trans. Microw. Theory Techn.*, vol. 57, no. 12, pp. 2948–2957, Dec. 2009.

[39] B. Yassini, M. Yu, and B. Keats, "A Ka-band fully tunable cavity filter," *IEEE Trans. Microw. Theory Techn.*, vol. 60, no. 12, pp. 4002–4012, Dec. 2012.

[40] S. Nam, B. Lee, C. Kwak, and J. Lee, "A new class of K-band high-Q frequency-tunable circular cavity filter," *IEEE Trans. Microw. Theory Techn.*, vol. 66, no. 3, pp. 1228–1237, Mar. 2018.

[41] S. Nam, B. Lee, C. Kwak, and J. Lee, "Contactless tuning plunger and its application to K-band frequency-tunable cavity filter," *IEEE Trans. Microw. Theory Techn.*, vol. 67, no. 7, pp. 2713–2719, Jul. 2019.

[42] M. Yu and A. Atia, "High power issues of microwave filter design and realization," in *IEEE MTT-S Int. Microw. Symp. Dig.*, Jun. 2007.

[43] C. Vicente and H. L. Hartagel, "Passive-intermodulation analysis between rough rectangular waveguide flanges," *IEEE Trans. Microw. Theory Techn.*, vol. 53, no. 8, pp. 2515–2525, Aug. 2005.

[44] K. N. Patel and M. R. Clark, "RF cavity resonator with low passive inter-modulation tuning element," U.S. Patent 10 845 167, Jul. 18, 2006.

[45] D. Smacchia et al., "Advanced compact setups for passive intermodulation measurements of satellite hardware," *IEEE Trans. Microw. Theory Techn.*, vol. 66, no. 2, pp. 700–710, Feb. 2018.
[46] C. Carceller, P. Soto, V. Boria, M. Guglielmi, and J. Gil, "Design of compact wideband manifold-coupled multiplexers," *IEEE Trans. Microw. Theory Techn.*, vol. 63, no. 10, pp. 3398–3407, Oct. 2015.
[47] W.-C. Tang and C. M. Kudsia, "Multipactor breakdown and passive intermodulation in microwave equipment for stellite applications," in *Proc. IEEE Conf. Mil. Commun.*, Oct. 1990, pp. 181–187.
[48] P. L. Lui, "Passive intermodulation interference in communication systems," *Electron. Commun. Eng. J.*, vol. 2, no. 3, pp. 109–118, Jun. 1990.
[49] V. E. Boria, M. Guglielmi, and T. Tronser, "Dielectric tuner," Spanish Patent 202 030 640 A Jun. 25, 2020.
[50] J. Saucourt et al., "Design of 3D printed plastic modular filters," in *Proc. 46th Eur. Microw. Conf. (EuMC)*, Oct. 2016, pp. 369–372.

Abhishek Sharma was born in New Delhi, India, in 1992. He received the bachelor's degree in electronics and communication from the Technical University of Uttar Pradesh, Lucknow, India, in 2014, and the master's degree in microwave and optical communication from the Department of Electronics and Communication, Delhi Technological University (formerly DCE), New Delhi, in 2017. He is currently pursuing the Ph.D. degree at the Microwave Applications Group (GAM-ITEAM), Universitat Politècnica de València (UPV), Valencia, Spain, like an Early Stage Researcher of the TESLA Network.

From 2017 to 2019, he was an RF design Engineer with the Microwave Component Division, Bharat Electronics Limited, Ghaziabad, India, under the Ministry of Defense of India, where he participated in the design of TR modules for active phased arrays and radars. During the Ph.D. degree, he has developed novel compact solutions for reconfigurable waveguide filters and multiplexers. His research interests include high-power filter design, reconfigurable filters, transmit–receive modules, RF subsystems, and radars.

Javier Ossorio was born in Valencia, Spain, in March 1992. He received the bachelor's degree in telecommunications and the double master's degree in telecommunications engineering from the Universitat Politècnica de València, Valencia, in 2014 and 2016, respectively, and the Ph.D. degree in telecommunications from the GAM iTEAM Group, Universitat Politècnica de València, in 2021.

In 2019, he joined the European Space Agency (ESA)-Val Space Consortium (VSC) European High Power RF Space Laboratory, Valencia. His current research interests include electromagnetic (EM) simulations, efficient design and optimizations of waveguide filters, and development of new tunable structure filters for satellite applications.

Davide Smacchia was born in Fano, Italy, in 1982. He received the B.Sc. and M.Sc. (cum laude) degrees in electronic engineering from the Università di Perugia, Perugia, Italy, in 2005 and 2008, respectively, and the Ph.D. degree (cum laude) in telecommunications engineering from the Universitat Politècnica de València, Valencia, Spain, in 2022.

From 2008 to 2010, he was a Researcher with the Departamento de Comunicaciones, Universidad Politècnica de València, granted by a Generalitat Valenciana Santiago Grisolía Fellowship. In 2010, he joined the European Space Agency (ESA)-Val Space Consortium (VSC) European High Power RF Space Laboratory, Valencia. His research interests include RF breakdown phenomena, such as multipactor and corona, as well as the analysis and measurement of passive intermodulation (PIM) for both conducted and radiated scenarios.

Dr. Smacchia is member of the Val Space Consortium Research and Development Board and the Technical Committee of the International Workshop on Multipactor, Corona and Passive Intermodulation (Mulcopim).

Tillmann Tronser was born in Pforzheim, Germany, in April 14, 1990. He received the B.S. degree in engineering and international management from the Pforzheim University of Applied Science, Pforzheim, in 2015.

After graduation, he joined the family business which has over 60 years of experience in manufacturing the highest quality variable capacitors as well as customized RF components. After implementing a new ERP-System in the company, he took over the Sales Department for the variable capacitors and custom RF components and became an Executive Vice President. He successfully revitalized this branch and gained substantial market share. In 2020, he split off the variable capacitor and custom RF component branch of the company to fully focus all of the efforts on these markets. He is currently the CEO of Tronser GmbH, Engelsbrand, Germany, as well as a Board Member and the Vice President of Alfred Tronser GmbH.

Santiago Cogollos (Member, IEEE) was born in Valencia, Spain, in 1972. He received the "Ingeniero Superior de Telecomunicación" and "Doctor Ingeniero de Telecomunicación" degrees from the Universitat Politècnica de València (UPV), Valencia, in 1996 and 2002, respectively.

In 2000, he joined the Communications Department, Universitat Politècnica de València, where he was an Assistant Lecturer from 2000 to 2001, a Lecturer from 2001 to 2002, an Associate Professor in 2002, and became a Full Professor in 2022. He has collaborated with the European Space Research and Technology Centre, European Space Agency, Valencia, in the development of modal analysis tools for payload systems in satellites. In 2005, he held a post-doctoral research position working in the area of new synthesis techniques in filter design at the University of Waterloo, Waterloo, ON, Canada. His current research interests include applied electromagnetics, mathematical methods for electromagnetic theory, analytical and numerical methods for the analysis of microwave structures, and design of waveguide components for space applications.

Vicente E. Boria (Fellow, IEEE) was born in Valencia, Spain, in May 1970. He received the Ingeniero de Telecomunicación (Hons.) and Doctor Ingeniero de Telecomunicación degrees from the Universidad Politècnica de València, Valencia, in 1993 and 1997, respectively.

In 1993, he joined the Departamento de Comunicaciones, Universidad Politècnica de València, where he has been a Full Professor, since 2003. In 1995 and 1996, he was holding a Spanish trainee position with the European Space Research and Technology Centre, European Space Agency (ESTEC-ESA), Noordwijk, The Netherlands, where he was involved in the area of EM analysis and design of passive waveguide devices. He has authored or coauthored ten chapters in technical textbooks, 180 articles in refereed international technical journals, and over 200 articles in international conference proceedings. His current research interests include the analysis and automated design of passive components, left-handed and periodic structures, and the simulation and measurement of power effects in passive waveguide systems.

Dr. Boria has been a member of the IEEE Microwave Theory and Techniques Society (IEEE MTT-S) and the IEEE Antennas and Propagation Society (IEEE AP-S) since 1992. He is also a member of the European Microwave Association (EuMA). He is also a member of the Technical Committees of the IEEE-MTT International Microwave Symposium and the European Microwave Conference. He also serves as an Editorial Board Member of the *International Journal of RF and Microwave Computer-Aided Engineering*. He has been the Chair for the 48th European Microwave Conference held in Madrid, Spain. He acts as a regular reviewer for the most relevant IEEE and IET technical journals on his areas of interest. He was an Associate Editor of the IEEE MICROWAVE AND WIRELESS COMPONENTS LETTERS from 2013 to 2018 and the *IET of Electronics Letters* from 2015 to 2018. He serves as a Subject Editor for *Microwaves Journal* and the *IET of Electronics Letters*.

Marco Guglielmi (Life Fellow, IEEE) was born in Rome, Italy, in December 1954. He received the "Laurea in Ingegneria Elettronica" degree from the University of Rome "La Sapienza," Rome, in 1979, the M.S. degree in electrical engineering from the University of Bridgeport, Bridgeport, CT, USA, in 1982, and the Ph.D. degree in electrophysics from Polytechnic University, Brooklyn, NY, USA, in 1986.

He also attended the Scuola di Specializzazione in Elettromagnetismo Applicato, University of Rome "La Sapienza," in 1980. From 1984 to 1986, he was an Academic Associate at Polytechnic University, where he was an Assistant Professor from 1986 to 1988. From 1988 to 1989, he was an Assistant Professor at the New Jersey Institute of Technology, Newark, NJ, USA. In 1989, he joined the RF System Division, European Space Agency, European Space Research and Technology Centre (ESTEC), Noordwijk, The Netherlands, as a Senior Microwave Engineer, where he was in charge of the development of microwave filters and electromagnetic simulation tools. In 2001, he was appointed as the Head of the Technology Strategy Section, ESTEC, where he contributed to the development of management processes and tools for the formulation of a European Strategy for Space Technology Research and Development. In 1981, he was awarded a Fulbright Scholarship in Rome and a Halsey International Scholarship Program (HISP) from the University of Bridgeport. In 2014, he retired from the European Space Agency and is currently an Invited Senior Researcher at the Polytechnic University of Valencia, Valencia, Spain.

Dr. Guglielmi has been elevated to the grade of a Fellow of the IEEE "For Contributions to Multimode Equivalent Networks and Microwave Filter Design," in January 2013.